CHEMISTRY
A EUROPEAN JOURNAL

DOI: 10.1002/chem.200700166

Buffering Dissociation/Formation Reaction of Biogenic Calcium Carbonate

Kazuhiko Ichikawa*[a]

Abstract: The oscillating stability of coral reef seawater pH has been maintained at around physiological pH values over the past 300 years (Pelejero et al., 2005). The stability mechanism of its pH has been interpreted in terms of the buffering dissolution/formation reaction of $CaCO_3$ as well as the proton consumption/generation reaction in $CaCO_3$-saturated water. Here the pH-dependent solubility product $[HCO_3^-][Ca^{2+}]$ has been derived on the basis of the actual pH-dependent reactions for the atmospheric $CO_2/CO_{2(aq.)}/HCO_3^-/CO_3^{2-}/Ca^{2+}/CaCO_3$ system. Overbasic pH peaks appeared between pH≈8 and ≈9.5 during sodium hydroxide titration, as a result of simultaneous $CaCO_3$ formation and proton generation. The spontaneous and prompt water pH recovery from the acidic to the physiological range has been confirmed by the observation of acid/base time evolution, because of simultaneous $CaCO_3$ dissolution and proton consumption. The dissolution/formation of $CaCO_3$ in water at pH 7.5–9 does not take place without a proton consumption/generation reaction, or a buffering chemical reaction of $HCO_3^-+Ca^{2+}\rightleftarrows CaCO_3+H^+$. SEM images of the $CaCO_3$ fragments showed that the acid water ate away at the $CaCO_3$ formed at physiological pH values. Natural coral reefs can thus recover the physiological pH levels of seawater from the acidic range through partial dissolution of their own skeletons.

Keywords: buffer action · calcium · carbon dioxide fixation · carbonates · coral reefs · solubility product

Introduction

Everybody recognizes that one of the most crucial seawater properties for marine organisms is the proton concentration. The pH of seawater inhabited by calcareous organisms is the master variable of the atmospheric $CO_2/CO_{2(aq.)}/HCO_3^-/CO_3^{2-}/Ca^{2+}$/biogenic $CaCO_3$ system. The pH of the seawater influences the calcareous organisms and probably make a great impact on oceanic CO_2 uptake. The variability of coral reef seawater pH over the 300 years prior to 1990 has been determined.[1] The boron isotope composition change ($\delta^{11}B$) method[2,3] was adapted for long-lived massive corals[1,4] or foraminifera.[5–8] The relative abundance of boric acid and borate in biogenic calcium carbonate is dependent on the seawater pH and should be governed by the standard affinity[9] of the acid dissociation reaction between the two boron chemical species.

Seawater has never recently experienced such a serious fall in pH levels as at the present time, and this could therefore be dangerous for the life and prosperity of calcareous organisms. The anthropogenic increase in carbon dioxide concentrations has sometimes been observed in the atmosphere. As the $CaCO_3$-based coral skeletons and shells dissolve in acid seawaters, it will become difficult for corals and calcareous planktons to maintain their own lives. The oscillating stability of the rising and falling ocean pH levels over the past 300 years[1] is certainly related to the biogenic calcium carbonate of natural coral reefs.

This article reveals the mechanism of the oscillating seawater pH stability—or the $CO_2/CO_{2(aq.)}/HCO_3^-/CO_3^{2-}/Ca^{2+}/CaCO_3$ system—developed by coral reef seawaters. The mechanism can be described in terms of the buffering dissolution/formation equation of biogenic $CaCO_3$. The equation is different from the pH-independent equation $CaCO_3\rightleftarrows CO_3^{2-}+Ca^{2+}$. It has been confirmed by acid–base titration experimentation that the dissolution/formation of $CaCO_3$ in water shows a buffer action and a pH-dependent reaction. The spontaneous recovery from acidic-range water to physiological range water and the oscillating stability of

[a] Prof. Dr. K. Ichikawa
Graduate School of Environmental Earth Science
Hokkaido University, Sapporo 060-0810 (Japan)
Fax: (+86) 11-706-9133
E-mail: ichikawa@ees.hokudai.ac.jp

Supporting information for this article is available on the WWW under http://www.chemeurj.org/ or from the author: SEM image of a paste-like $CaCO_3$ fragment obtained from a Ca^{2+} solution (5 mM) including $NaHCO_3$ (0.1 M) in a stationary state after the spontaneous recovery from acidic water: pH≈4 to pH≈7.2. The water at pH≈4 ate away at the fragment.

water pH are discussed from the point of view of the buffering formation/dissolution reaction of $CaCO_3$ in the saturated water.

Results and Discussion

Overbasic pH peak appearance during sodium hydroxide titration: An "overbasic" pH peak appeared between pH≈8 and ≈9.5 in the course of sodium hydroxide titration into NaX (0.1 M) and Ca^{2+} (5 mM) solution at pH≈5, where NaX is NaCl (thick curve), or $NaNO_3$ or $NaHCO_3$ (Figure 1). The

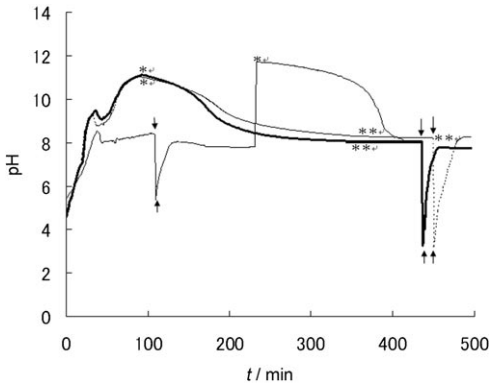

Figure 1. Time evolution of proton concentration for the $CO_2/CO_{2(aq.)}/HCO_3^-/CO_3^{2-}/Ca^{2+}/CaCO_3$ system measured during NaOH (0.05 M) titration into Ca^{2+} (5 mM) including NaCl (0.1 M, thick curve), $NaNO_3$, or $NaHCO_3$ solution with vigorous stirring: An overbasic pH peak appeared between pH 8 and 9.5 during the sodium hydroxide titration in each case. The overbasic peaks were observed at lower pH (≈8.5) for $NaHCO_3$ solution (0.1 M) and at higher pH (≈9.5) for NaCl (thick curve) or $NaNO_3$. At the down arrows HNO_3 was quickly added to these solutions to keep the pH at 4–6. At the up arrows the HNO_3 addition was stopped and the spontaneous recovery from acidic to physiological was observed with vigorous stirring. Between * and ** the NaCl (thick curve) and $NaNO_3$ solutions showed spontaneous recovery from the basic to the physiological ranges after NaOH titration was stopped at pH≈11.5.

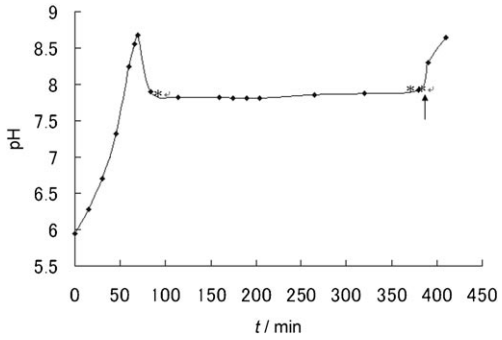

Figure 2. Time evolution of proton concentration in the $CO_2/CO_{2(aq.)}/HCO_3^-/CO_3^{2-}/Ca^{2+}/CaCO_3$ system measured during NaOH (0.05 M) titration into Ca^{2+} solution (5 mM) including $NaNO_3$ (0.1 M): When the sodium hydroxide titration was immediately stopped directly after an observed pH peak, the $CaCO_3$-suspended solution pH of ≈8.7 relaxed to a physiological pH of ≈8. A stationary state or a nearly equilibrium state appeared between * and ** after the starting of the NaOH titration at an up arrow.

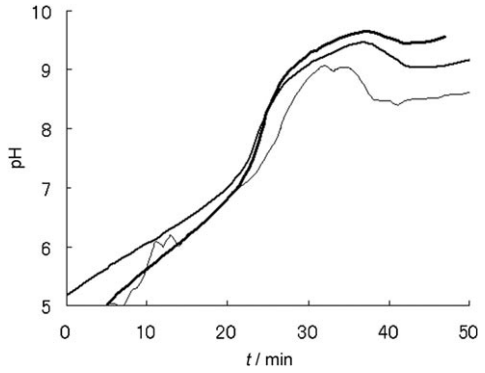

Figure 3. Calcium concentration dependence of superbasic pH peaks was measured by NaOH titration (0.05 M) into $CaNO_3$ solutions [3 mM (thick curve), 5 mM (intermediate curve), or 10 mM (thin curve)] including NaCl (0.1 M). The sharper peaks were observed at the lower pH values with increasing Ca^{2+} concentrations. In the absence of Ca^{2+} no superbasic pH peak was ever detected during the NaOH titration.

pH peak appearance followed opalescence caused by the nucleation of $CaCO_3$ immediately before its precipitation, as confirmed by the naked eye. After the overbasic pH peak had been observed and the sodium hydroxide titration had been stopped, the $CaCO_3$-suspended solution relaxed to a stationary state or a nearly equilibrium state at physiological pH≈8 (Figure 2). Simultaneous pH decrease and $CaCO_3$ precipitation were clearly observed between pH 8 and 9.5 during the sodium hydroxide titration. The slower $CaCO_3$ formation reaction between HCO_3^- and Ca^{2+} gave rise to the falling water pH levels (i.e., the overbasic pH peaks; Figures 1 and 2). The $CaCO_3$ formation thus generates protons as a product of the acid dissociation reaction of Ca^{2+}-recognized HCO_3^-.

The intensity, profile, and pH region of the observed overbasic pH peaks depended on $[HCO_3^-]$ (Figure 1) and $[Ca^{2+}]$ (Figure 3) and on the hydroxide titration rate. For the aqueous $NaHCO_3$ (0.1 M) of the higher HCO_3^- concentration the overbasic peak was observed at the lower pH (≈8.5). For NaCl (0.1 M, thick curve) or $NaNO_3$ solution, on the other hand, the peaks were located at the higher pH values of 8.5–9.5, because of their lower $[HCO_3^-]$ values and the pH dependence of the solubility product $[HCO_3^-][Ca^{2+}]$, as discussed later.

The chemical reaction equations, Equations (1)–(5) and (7), shown in Table 1 may be coupled to one another for the $CO_2/CO_{2(aq.)}/HCO_3^-/CO_3^{2-}/Ca^{2+}/CaCO_3$ system. The positive/negative standard affinity (A_o) at atmospheric pressure and room temperature, as shown on the right-hand side of Table 1, indicates the tendencies toward the right-/left-hand sides of Equations (1)–(7). These are numerically the same as the standard Gibbs free energy changes ($\Delta G^\ominus$) of the equations, although they are of opposite sign.[9]

The equilibrium state of acid–base reactions with large A_o can be reached right after the addition of OH^-/H^+. For the positive A_o the right-hand components are major and the

Table 1. All possible reactions as chemical equations coupled to each other for the $CO_2/CO_{2(aq.)}/HCO_3^-/CO_3^{2-}/Ca^{2+}/CaCO_3$ system.

equation for dissolved $CO_{2(aq.)}$ in equilibrium with atmospheric CO_2:		
$CO_2 \rightleftarrows CO_{2(aq.)}$	$A_o = -8.5\ kJ\,mol^{-1}$	(1)
neutralization reaction equation:		
$H^+ + OH^- \rightleftarrows H_2O$	79.9	(2)
$CO_{2(aq.)}$ nucleophilic reaction equation:		
$CO_{2(aq.)} + OH^- \rightleftarrows HCO_3^-$	43.7	(3)
calcium carbonate formation/dissolution reaction or acid dissociation reaction equation of Ca^{2+}-induced HCO_3^-:		
$HCO_3^- + Ca^{2+} \rightleftarrows CaCO_3 + H^+$	−11.7	(4)
the well known first acid dissociation equilibrium equation:		
$CO_2 + H_2O \rightleftarrows HCO_3^- + H^+$	−44.7	(5)
and the second acid dissociation reaction equation:		
$HCO_3^- \rightleftarrows CO_3^{2-} + H^+$	−59.5	(6)
calcium carbonate formation/dissolution equilibrium equation:		
$CO_3^{2-} + Ca^{2+} \rightleftarrows CaCO_3$	47.4	(7)

left-hand components minor [e.g., Equations (2), (3), and (7)], as the right-hand sides are much more stable than the left in view of their standard Gibbs free energies. For negative A_o, vice versa [Eqs. (5) and (6)].

The addition of strong base forms the chemical species HCO_3^- through a $CO_{2(aq.)}$ nucleophilic reaction [Eq. (3)] and a CO_2 dissolution reaction [Eq. (1)], because of the large value of A_o for Equation (3). The simultaneous reactions of the acid dissociation of the Ca^{2+}-induced HCO_3^- and the $CaCO_3$ formation may have a delay time because of a negative and small absolute value of A_o for Equation (4).

Both the Ca^{2+}-induced acid dissociation of the formed HCO_3^- of Equation (3) and the $CaCO_3$ precipitation take place simultaneously between the major species: HCO_3^- and Ca^{2+} [see Eq. (4)]

Here, the HCO_3^- formation and the consumption of titrated hydroxide ions takes place through the $CO_{2(aq.)}$ nucleophilic reaction of Equation (3). The acid dissociation constant (pK_a) of Ca^{2+}-induced HCO_3^- is much less than pK_a (10.3) of HCO_3^- in Equation (6) with no calcium ions, as estimated later. Since the $[CO_3^{2-}]/[HCO_3^-]$ ratio between pH 7.5 and 9.5 is extremely small (i.e., 5×10^{-4}–5×10^{-2}), the well known equation of Equation (7) may practically not contribute to the $CaCO_3$ formation in this pH region. Each of the concentration fractions of the chemical species $CO_{2(aq.)}$, HCO_3^-, and CO_3^{2-} was evaluated from the acid dissociation constants of Equations (5) and (6) at a given pH.[10]

For the marine calcareous organisms, the HCO_3^- species are formed through enzymatic OH^- nucleophilic reactions of CO_2.[11–13] The calcification or acid dissociation of HCO_3^- may be carried out through $HCO_3^- + Ca^{2+} \rightarrow CaCO_3 + H^+$ at the Ca^{2+}-recognizing sites of the acidic amino acid residues of the matrix protein,[14,15] the tertrates/glycoxylates of polysaccharide,[16] and the carboxylates of polyaspartate as a biomimetic.[17] The formed protons may be pulled out of the cells and may contribute to photosynthesis and respiration of the marine calcareous organisms.

Spontaneous recovery of the pH of $CaCO_3$-saturated water from the acidic to the physiological range: The spontaneous pH recovery from pH 4–6 to around 8 started at the up arrows (Figure 1) after acidification of the $CaCO_3$-suspended water to pH 4–6 by use of HNO_3 at the down arrows. The $CaCO_3$ mass was dependent on the water pH because of the decreased solubility product $[HCO_3^-][Ca^{2+}]$ with increasing pH, as shown later. The spontaneous acidic decrease from pH 4–6 to pH ≈ 8 progressed through proton consumption owing to the $CaCO_3$ dissolution reaction,

$$CaCO_3 + H^+ \rightarrow HCO_3^- + Ca^{2+} \quad (8)$$

The $CaCO_3$-saturated water had shortly reached the stationary state at physiological pH ≈ 8 after half an hour had passed (the up arrows in Figure 1).

The standard affinity (A_o) of the $CaCO_3$ dissolution reaction is given by

$$A_o = A_{o,f}(HCO_3^-) + A_{o,f}(Ca^{2+}) - A_{o,f}(CaCO_3) - A_{o,f}(H^+) \quad (9)$$

where $A_{o,f}(i)$ stands for the standard affinity of the chemical species i in the $CaCO_3$ formation reaction. It is numerically the same as its standard Gibbs free energy of formation reaction, although it has the opposite sign.[9] The small but positive A_o of 11.7 kJ mol^{-1} indicates the tendency toward the dissolution reaction of saturated $CaCO_3$, and the HCO_3^- species are predominant among the chemical species $CO_{2(aq.)}$, HCO_{3-} and CO_3^{2-} between 7.5 and 9. On the other hand, the pH-independent $CaCO_3$ dissolution reaction—$CaCO_3 \rightarrow Ca^{2+} + CO_3^{2-}$—is inhibited because $A_o = -47.4\ kJ\,mol^{-1}$ at 300 K; the solubility product $[Ca^{2+}][CO_3^{2-}] = \approx 6\times10^{-9}\ M^2$ at room temperature and atmospheric pressure. Water at pH ≈ 11 or ≈ 12 showed spontaneous pH recovery to water at pH ≈ 8 through the absorption of atmospheric CO_2 between * and ** in Figure 1; it took ca. four hours to reach a stationary state at pH ≈ 8.

$CaCO_3$ fragments were formed after i) NaOH titration up to pH ≈ 12, ii) HNO_3 (0.1 M) titration from pH ≈ 12 to pH ≈ 6, and iii) spontaneous recovery from pH ≈ 6 to pH ≈ 7.5. The morphology of $CaCO_3$ changed from a number of fine species precipitated at pH 8–9.5 to a $CaCO_3$ fragment. A SEM image of a $CaCO_3$ fragment of around $5\times5\ mm^2$ (Figure 4) is reminiscent of the $CaCO_3$ shell of a living zooplankton pteropod after advanced dissolution after exposure to acid water.[18] The calcium carbonate polymorphs were qualitatively assigned to aragonite and calcite from the observed X-ray diffraction patterns[17] of the $CaCO_3$ fragment

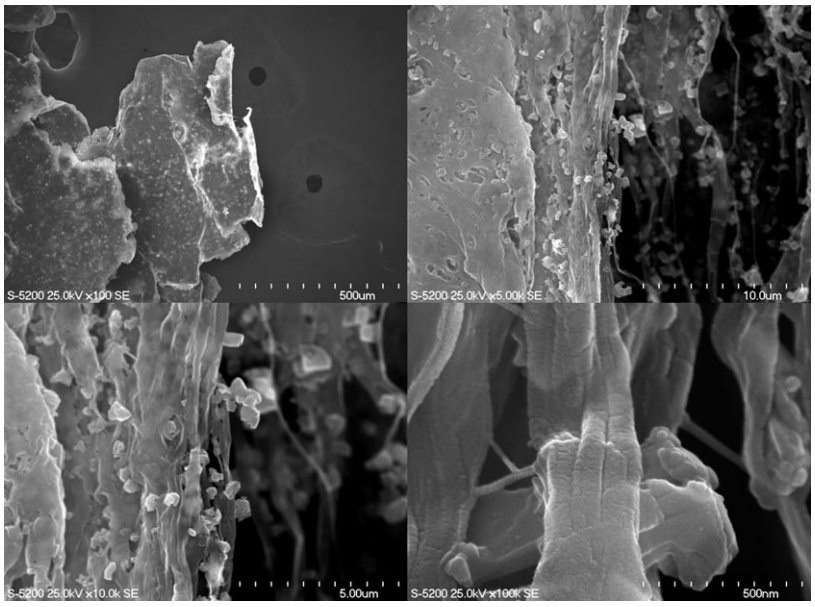

Figure 4. Scanning electron microscopy (SEM) image of a $CaCO_3$ fragment (around $5\times5\,mm^2$) obtained from Ca^{2+} (5 mM) solution including $NaHCO_3$ (0.1 M) at a stationary state after spontaneous recovery from acidic water pH≈6 to pH≈7.5. The other three SEM images are at higher magnification. Crystalline particles (around $0.5^3\,\mu m^3$) were scattered in the paste-like $CaCO_3$ matrix.

shown in the SEM image (Figure 4). A different, paste-like $CaCO_3$ fragment was obtained from Ca^{2+} (5 mM) including $NaHCO_3$ solution (0.1 M) at pH≈7.2 after spontaneous recovery from pH≈4. The SEM image demonstrated that acidic water of pH≈4 ate away at the fragment more markedly (Figure S in the Supporting Information).

The $CaCO_3$ dissolution/formation mechanism is different from that of water-soluble alkali metal halide MX. Protonated water molecules (i.e., hydronium ions) react with the lattice site of CO_3^{2-} to form HCO_3^- in the double atomic layers at the interface of crystalline $CaCO_3$ and acid water. The incompletely hydrated HCO_3^- in the double atomic layers can dissolve in water because it is less stable than the completely hydrated HCO_3^-. The $CaCO_3$ dissolution associated with the proton consumption induced the decrease in acidity from pH 4–6 to the physiological pH range (≈8). The XPS C_{1s} spectrum from humidity-exposed calcite suggested the very weak shoulder assigned to HCO_3^- at the higher binding energy side of the main peak of CO_3^{2-}.[19] The FT-IR difference spectrum of $CaCO_3$ particles in the vapor phase of HNO_3 showed the negative band at 1598 cm^{-1} assigned to the adsorbed HCO_3^-.[20] The dissolution mechanism of water-soluble alkali halides MX, on the other hand, were revealed from the observed AFM images. This demonstrated the metastable structures built up by intermolecular interactions between the point-charge M^+/X^- and the dipole H_2O at the crystal/water interface.[21,22] The Na^+/K^+ ions of the NaCl/KBr side of the double atomic layers are pulled up from their own lattice sites into the water layer by the intermolecular interaction between Na^+ and water molecule without any chemical reaction, such as protonation.

The buffering dissolution/formation reaction of biogenic $CaCO_3$ and the acid dissociation reaction of Ca^{2+}-induced HCO_3^-: A dynamic equilibrium equation between calcification and acid dissociation of Ca^{2+}-derived HCO_3^- can be written down as $HCO_3^- + Ca^{2+} \rightleftarrows CaCO_3 + H^+$. Its equilibrium constant corresponds to the acid dissociation constant (K_a) of Ca^{2+}-recognized HCO_3^-: $K_a = [H^+]/([HCO_3^-][Ca^{2+}])$. The solubility product $[HCO_3^-][Ca^{2+}]$ ($=X_{sp}$) thus depends on water pH as a master variable because of $\log(X_{sp}) = pK_a - pH$; pK_a can be estimated from the four standard free energy changes of the formation reactions of HCO_3^-, Ca^{2+}, $CaCO_3$, and H^+. The estimated pK_a is equal to 2.0 at 300 K and 1 atm because of the standard Gibbs free energy change ($\Delta G^\ominus = 11.7\,kJ\,mol^{-1}$) of the above equilibrium equation or Equation (4) in Table 1. Both the $CaCO_3$ formation and its dissolution can slowly progress under the effect of water pH change on $[HCO_3^-][Ca^{2+}]$ because of the small and positive $\Delta G^\ominus$. The calcium carbonate is soluble in acid water, but only slightly soluble in physiological water: X is equal to $\approx10^{-4}\,M^2$ at pH 6 and $\approx10^{-6}\,M^2$ at physiological pH 8 according to $\log(X_{sp}) = pK_a - pH$. The solubility of $CaCO_3$ in the acidic water is about 100 times higher than in physiological water. Here, a rise in the water pH and fall in X_{sp} can be derived from the saturated $CaCO_3$ dissolution. The $CaCO_3$-saturated water is thus likely to be modulated toward the physiological-range water from the acid-range water. The observed spontaneous and prompt pH recovery from acid-range water to physiological-range water has occurred as a result of the simultaneous rise in pH (see the up arrows of Figure 1) and fall in X_{sp} for the $CO_{2(aq.)}/HCO_3^-/CO_3^{2-}/Ca^{2+}/CaCO_3$ system. The $CaCO_3$-saturated water at pH < 9.5 can act a pH buffer. The pH-independent $CaCO_3$ dissolution through an equilibrium equation $CaCO_3 \rightleftarrows CO_3^{2-} + Ca^{2+}$ may take place at pH > 9.5. The dissolution process, however, is almost inhibited because of the large and positive $\Delta G^\ominus = 47.4\,kJ\,mol^{-1}$.

As the pK_{a2} of hydrated HCO_3^-, or the equilibrium constant of $HCO_3^- \rightleftarrows CO_3^{2-} + H^+$, in the absence of Ca^{2+} at 300 K is equal to 10.3,[10] the remarkable pK_a decrease to 2.0 in the presence of Ca^{2+} may be assessed by the fact that the interaction of Ca^{2+} with HCO_3^- accelerates its acid dissociation. Zinc-coordinated water molecules ($H_2O\cdots Zn^{2+}$) show a marked decrease from pH 14 to 7–9; zinc-coordinated water molecules could be operative at each active site of carbonic anhydrase/nacrein[11] and zinc complex/array mimics.[12,17,23]

Impact of seawater acidification on calcareous organisms and ocean CO_2 uptake: Seawater from natural coral reefs and the calcareous plankton-inhabited ocean may be simplified to the $CO_2/CO_{2(aq.)}/HCO_3^-/CO_3^{2-}/Ca^{2+}/CaCO_3$ system at pH 7.5–9. Firstly, acid ocean conditions at $pH < 6.5$ eat away at the $CaCO_3$-based skeletons of corals and the $CaCO_3$-based outer casings of the calcareous foraminifera and coccolithophores that form the basis of food webs.[18,24–26] Secondly, anthropogenic ocean acidification has a serious impact on ocean CO_2 uptake because of the pH-dependent solubility (S) of atmospheric CO_2: $S = [CO_{2(aq.)}] + [HCO_3^-]$ at $pH < 9$ corresponds to $S = (1 + 10^{pH-pKa1}) \times [CO_{2(aq.)}]$, where pK_{a1} is equal to the acid dissociation constant of $CO_{2(aq.)} + H_2O \rightleftarrows HCO_3^- + H^+$ ($pK_{a1} = 6.4$ at 300 K). The solubility of CO_2 in physiological-range seawater is about 100 times greater than in acid-range seawater: $S \approx 2 \times [CO_{2(aq.)}]$ at pH 6.5 and $S \approx 101 \times [CO_{2(aq.)}]$ at pH 8.5.

It may be pointed out that anthropogenic ocean acidification has been progressing since the end of the twentieth century. The SOx and NOx released to the atmosphere is dissolved into seawaters as acidic rain of pH 4–5. A serious impact on calcareous organisms may be inferred in future because of the one hundred times larger $[HCO_3^-][Ca^{2+}]$ ($= 10^{pKa-pH} = 10^{2.0-pH}$, as mentioned above) through the decrease in pH from the physiological pH 8 to the acidic pH 6. The $CaCO_3$-undersaturated seawaters would not be able to recover from the acidic to the physiological range.

The acidic ups and downs of seawater inhabited by calcareous organisms could progress along with $CaCO_3$ formation/dissolution in response to the pH-dependent $[HCO_3^-][Ca^{2+}]$ under the equilibrium between atmospheric CO_2 and $CO_{2(aq.)}$. The natural oceanic pH could be governed by the buffer action chemistry of biogenic $CaCO_3$, as mentioned above, and calcareous organisms have certainly lessened the greenhouse effect.[27,28] The calcification of marine planktons has been reduced in acidic ocean conditions as a result of the higher partial pressure of atmospheric CO_2.[18,24–26] Oceanic acidification could amplify global warming because of the deceased total dissolved carbon in seawater.

The ecosystem inhabited by corals has preserved its pH in an oscillating stability between pH 7.9 and 8.2 in the large and long spatial-temporal environment of the past 300 years,[1] owing to the buffering formation/dissolution reaction of biogenic $CaCO_3$ in seawater. Here, the pH change from 8.2 to 7.9 corresponds to an increase in $[HCO_3^-][Ca^{2+}]$ of around twofold. The glacial–interglacial stability of oceanic pH may be governed by the biogenic $CaCO_3$ formed by massive foraminifera.[29] Since the physiological oceanic pH is fit for many different species of marine organisms, the coral reef ecosystem should be able to provide sustainable biodiversity.[30] Seawater inhabited by calcareous organisms can play a role in oceanic CO_2 uptake because of the higher solubility of atmospheric CO_2 through the formation of the major chemical species HCO_3^- at physiological pH.

Experimental Section

Materials: $NaHCO_3$ was obtained from Junsei. NaCl, $NaNO_3$, $Ca(NO_3)_2 \cdot 4H_2O$, and NaOH (0.1 M) and HNO_3 (0.1 M) solutions were obtained from Wako, and $CO_{2(g)}$ from Air Water. The commercial reagents were used as obtained without further purification.

pH titration: The pH/time evolution of solutions was determined by automatically measuring the pH every one minute during more than eight hours with vigorous stirring because of $CaCO_3$ precipitation by use of a pH meter (Nissin, CE-108C), a pH controller (Nissin, NPH-660 NDE), a roller pump (Nissin, NRP-75), and a magnetic stirrer (Finn, FS-05).

Acknowledgements

I gratefully acknowledge the stimulating and inspiring discussions with C. Pelejero and thank him for drawing attention to the many references relating to the oceanic pH effect on boron isotopic compositions in biogenic $CaCO_3$ formed by corals or foraminifera.

[1] C. Pelejero, E. Calvo, M. T. McCulloch, J. F. Marshall, M. K. Gága, J. M. Lough, B. N. Opdyke, *Science* **2005**, *309*, 2204–2207.
[2] N. G. Hemming, G. N. Hanson, *Geochim. Cosmochim. Acta* **1992**, *56*, 537–543.
[3] A. Sanyal, N. G. Hemming, W. S. Broecker, D. W. Lea, H. J. Spero, G. N. Hanson, *Paleoceanography* **1996**, *11*, 513–517.
[4] B. Hönisch, N. G. Hemming, A. G. Grottoli, A. Amat, G. N. Hanson, J. Bijmá, *Geochim. Cosmochim. Acta* **2004**, *68*, 3675–3685.
[5] A. Sanyal, N. G. Hemming, G. N. Hanson, W. S. Broecker, *Nature* **1995**, *373*, 234–236.
[6] P. N. Pearson, M. R. Palmer, *Science* **1999**, *284*, 1824–1826.
[7] R. E. Zeebe, *Geochim. Cosmochim. Acta* **2005**, 69, 2753–2766.
[8] B. Hönisch, N. G. Hemming, *Earth and Planet. Sci. Lett.* **2005**, *236*, 305–314.
[9] I. Prigogine, R. Defay, D. H. Everett, *Chemical Thermodynamics*, Longman, London, **1973**.
[10] see for example, S. E. Manahan, *Environmental Chemistry*, CRC Press, London, **1994**.
[11] H. Miyamoto, T. Miyashita, M. Okushima, S. Nakano, T. Morita, A. Matsushiro, *Proc. Natl. Acad. Sci. USA* **1996**, *93*, 9657–9660.
[12] K. Nakata, *J. Inorg. Biochem.* **2002**, *89*, 255–266.
[13] Y. Shiraiwa, *Comp. Biochem. Physiol. Part B* **2003**, *136*, 775–783.
[14] T. Samata, N. Hayashi, M. Kono, K. Hasegawa, C. Horita, S. Akera, *FEBS Lett.* **1999**, *462*, 225–229.
[15] M. Kono, N. Hayashi, T. Samata, *Biochem. Biophys. Res. Commun.* **2000**, *269*, 213–218.
[16] M. E. Marsh, *Comp. Biochem. Physiol. Part B* **2003**, *136*, 743–754.
[17] K. Ichikawa, N. Shimomura, M. Yamada, N. Ohkubo, *Chem. Eur. J.* **2003**, *9*, 3235–3241.
[18] J. C. Orr, V. J. Faby, O. Aumont, L. Bopp, S. C. Doney, R. A. Feely, A. Granadesikan, N. Grube, A. Ishida, F. Joos, R. M. Key, K. Lindsay, E. Maier-Reimer, R. Matear, P. Monfray, A. Mouchet, R. G. Najjar, G. Plattner, K. B. Rodgers, C. L. Sabine, J. L. Sarminento, R. Schlitzer, R. D. Slater, I. J. Totterdell, M. Weirig, Y. Yamanaka, A. Yool, *Nature* **2005**, *437*, 681–686.
[19] S. L. S. Stipp, *Geoochem. Cosmochimica. Acta* **1999**, *63*, 3121–3131.
[20] H. A. Al-Hosney, V. H. Grassian, *J. Am. Chem. Scc.* **2004**, *126*, 8068–8069.
[21] K. Ichikawa, S. Sato, N. Shimomura, *Pure Appl. Chem.* **2004**, *76*, 115–122.
[22] K. Ichikawa, M. Yamada, *J. Phys. Condens. Matter* **1996**, *8*, 4889–4901.
[23] K. Ichikawa, M. Tarnai, M. K. Uddin, K. Nakata, S. Sato, *J. Inorg. Biochem.* **2002**, *91*, 437–450.
[24] J. Ruttimann, *Nature* **2006**, 442, 978–980.

[25] R. A. Feely, C. L. Sábine, K. Lee, W. Berelson, J. Kleypas, V. J. Fabry, F. J. Millero, *Science* **2004**, *305*, 362–366.
[26] J. A. Kleypas, R. W. Buddemeier, D. Archer, J.-P. Gáttuso, C. Lángdon, B. N. Opdyke, *Science* **1999**, *284*, 118–120.
[27] S. Bains, R. D. Norris, R. M. Corfield, K. L. Faul, *Nature* **2000**, *407*, 171–173.
[28] B. Schmitz, *Nature* **2000**, *407*, 143–144.
[29] D. M. Anderson, D. Archer, *Nature* **2002**, *416*, 70–73.
[30] M. Dornelas, S. R. Connolly, T. P. Hughes, *Nature* **2006**, *440*, 80–82.

Received: January 31, 2007
Revised: June 12, 2007
Published online: October 1, 2007

